Molecular Orientation and Mechanical Properties of Poly(Vinyl Alcohol) Fibers

M. van Gurp[a]

[a] DSM Research, MD Geleen, The Netherlands

PLEASE SCROLL DOWN FOR ARTICLE

Molecular Orientation and Mechanical Properties of Poly(Vinyl Alcohol) Fibers

M. VAN GURP

DSM Research P.O. Box 18, 6160 MD Geleen, The Netherlands

A number of poly(vinyl alcohol) fibers with different draw ratios was characterized by measuring the birefringence, crystalline orientational order, crystallinity, tensile strength, and modulus. The birefringence, tensile strength and modulus increased with increasing draw ratio whereas the crystallinity and crystalline order parameters remained constant within narrow limits. The increase in birefringence has to be attributed solely to an increase in chain orientation in the amorphous phase of the semicrystalline fiber. The tensile strength and modulus are therefore directly related to the chain orientation in the amorphous phase. With the aid of a simple two-phase model it was found that the modulus of the amorphous phase in its disordered conformation was 4.8 GPa. The intrinsic birefringence of the amorphous phase was found to be 79×10^{-3}, i.e. much higher than the value obtained for the crystalline phase (52×10^{-3}). When this value was used in calculations, it was found that the order parameter of the amorphous phase increased from around 0.1 for a draw ratio of 1 to approximately 0.6 for a draw ratio of 5, whereas the order parameter of the crystalline phase was close to 1 for all draw ratios.

KEY WORDS   Orientation, birefringence, intrinsic birefringence, amorphous orientation, mechanical properties, poly(vinyl alcohol).

INTRODUCTION

Poly(vinyl alcohol) (PVAL) fibers have been produced commercially for over four decades now. Scientific research on the structure and properties of these fibers has a correspondingly long history.[1] However, the invention of the so-called gel-spinning technique[2] has given new impulses to the production of PVAL fibers with improved mechanical properties.[3−6] These gel-spun, "high-performance" PVAL fibers appear to be attractive for applications in mechanical rubber goods and specialty tires. Especially mechanical properties such as tensile strength and fatigue are important in such applications.

In order to get a better understanding of the relations between the microscopic structure and the mechanical properties of gel-spun PVAL fibers, research was done on a number of fibers with differing draw ratios. Tensile tests were performed, along with structural characterization via birefringence, WAXS and DSC.

The present report discusses the results in the light of a two-phase crystalline-amorphous series model. The respective contributions of the two phases to the mechanical properties will be examined.

THEORETICAL BACKGROUND

The birefringence Δn of a semicrystalline polymer will in general be the total of three

components: Δn_c of the crystals, Δn_a of the amorphous phase and Δn_f of the interphase between crystalline and amorphous regions:

$$n = n_c + n_a + n_f. \tag{1}$$

This last component, the so-called form birefringence, is usually negligible. The contribution of the amorphous and crystalline components will depend on their respective volume fractions and average degree of chain orientation according to:[7]

$$n = \chi_c f_c n_c^0 + (1 - \chi_c) f_a n_a^0, \tag{2}$$

where χ_c is the volume fraction of crystalline material, f_c and f_a are the second rank order parameters of the crystalline and amorphous phases, respectively, and n_c^0 and n_a^0 are their respective intrinsic birefringence values. Similarly, the modulus of the material will be dependent on the modulus of the amorphous phase and that of the crystalline phase and their respective volume fractions. When the amorphous and crystalline phases are coupled in series we have:

$$\frac{1}{E} = \frac{\chi_c}{E_c} + \frac{1 - \chi_c}{E_a}, \tag{3}$$

where E_c and E_a are the moduli of both phases in the direction of drawing. In a very simple approximation the modulus of the amorphous phase can be expressed in terms of the modulus of isotropic amorphous material, E_{iso}, and the order parameter f_a according to:[8,9]

$$E_a = \frac{E_{iso}}{1 - f_a}. \tag{4}$$

The crystalline modulus E_c will also be orientation dependent. It is assumed that the aggregate model[10] applies, which relates the average modulus E_c to the individual crystal compliances:

$$\frac{1}{E_c} = S_{11} - (2S_{11} - 2S_{13} - S_{44})\langle\cos^2\Theta\rangle + (S_{11} + S_{33} - 2S_{13} - S_{44})\langle\cos^4\Theta\rangle, \tag{5}$$

where the average values $\langle\cos^2\Theta\rangle$ and $\langle\cos^4\Theta\rangle$ are related to the second- and fourth-rank order parameters $\langle P_2\rangle = (3\langle\cos^2\Theta\rangle - 1)/2 = f_c$ and $\langle P_4\rangle = (35\langle\cos^4\Theta\rangle - 30\langle\cos^2\Theta\rangle + 3)/8$ of the crystalline orientational distribution.

Equations (2)–(4) can be combined to directly relate the modulus and the birefringence:

$$\frac{1}{E} = a - bn, \tag{6}$$

where

$$a = \frac{\chi_c}{E_c} + \frac{1 - \chi_c}{E_{iso}} + \frac{\chi_c f_c n_c^0}{E_{iso} n_a^0},$$

$$b = \frac{1}{E_{iso} n_a^0}.$$

If the parameters χ_c, E_c, f_c, and n_c^0 do not change significantly in a series of experiments, a straight line is obtained when $1/E$ is plotted as a function of Δn. E_{iso} and Δn_a^0 can now be determined from the slope b and the intercept a if the other parameters are known. The order parameter f_a can then be determined from Equation (2) or from Equations (3) and (4).

EXPERIMENTAL SECTION

PVAL fibers

Spun PVAL yarn and one fully drawn yarn were kindly supplied by DSM High Performance Fibers BV. The spun yarn was stretched 1 to 5 times in a hot-air oven at a temperature of approximately 230°C.

Mechanical properties

The *dtex* of the fibers was determined by weighing. This value was then used to determine the cross sectional area on the assumption of a density of 1.32 g cm^{-3}. Tensile tests were carried out with the aid of a Zwick 1474 tensile tester equipped with fiber clamps to determine tensile modulus, strength and elongation at break. The distance between the grips was 20 cm, the crosshead speed was 10 cm/min and the modulus was determined between 0.2 and 0.5% elongation. The mechanical tests were performed immediately after drawing.

Shrinkage

Shrinkage experiments were carried out by immersing a portion of a 40 cm long yarn (5–10 monofilaments) in Lauda thermostat bath oil at 250°C for 30 s. The degree of shrinkage is defined as 40 cm divided by the length of the filaments after the experiment.

Crystallinity

The crystallinity was determined by means of a Perkin–Elmer DSC-2 at a heating rate of 10 deg min^{-1}. The crystallinity was taken to be the integrated melting enthalpy divided by 156 J g^{-1} (Reference 1).

Wide-angle X-ray diffraction

Wide-angle X-ray diffractograms were obtained with a Statton camera using a flat film geometry, with Ni-filtered CuK$_\alpha$-radiation generated by a Philips PW1729 generator operating at 50 kV and 40 mA. The photographically recorded X-ray patterns were scanned tangentially across the $(101)/(200)$ diffraction spots using an Enraf Nonius Microdensitometer. From the orientational distribution curve thus obtained the second- and fourth-rank order parameters of the crystallographic c direction were numerically calculated.

Birefringence

Birefringence measurements were carried out on a Zeiss standard Polarization Microscope fitted with an Ehringhaus compensator (magnification ×500). Table I gives the difference in optical path length corresponding to the tilting angle of the compensator. The birefringence was determined by dividing the optical path length by the thickness.
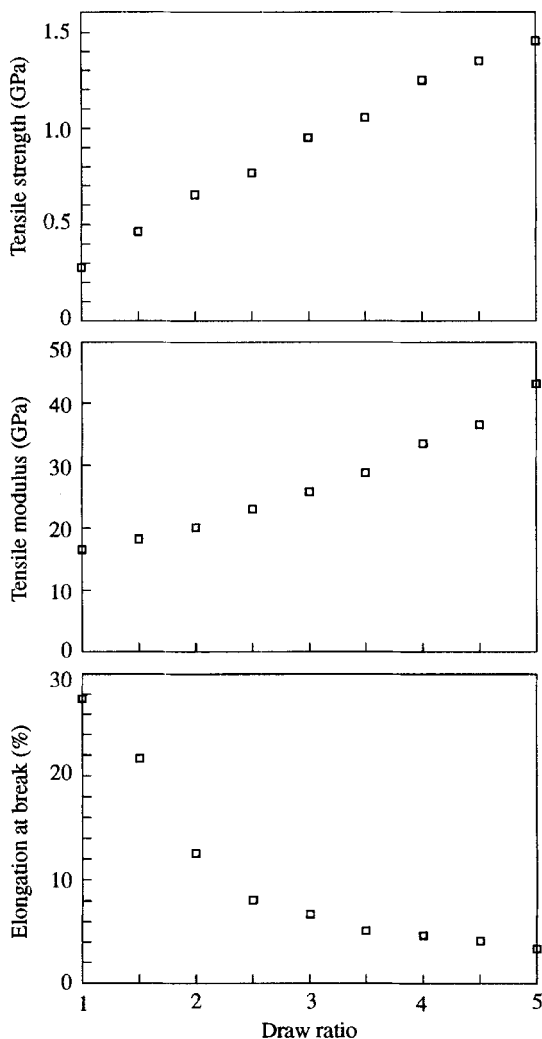
FIGURE 1   Tensile strength, tensile modulus and elongation at break as a function of the draw ratio in the oven.

RESULTS AND DISCUSSION

Experimental results

Figure 1 shows the tensile strength, modulus and elongation at break as functions of the draw ratio in the oven. The curves show the usual improvement of the mechanical properties with increasing degree of deformation. Figure 2 shows the degree of shrinkage as a function of the draw ratio. The spread in the measuring points reflects the inaccuracy of this measurement. Moreover, the fact that the fibers shrink very irregularly at high draw ratios in particular may have led to some systematic error.

Table I shows the crystallinity and (peak) melting temperature as derived from the DSC measurements. The crystallinity and melting temperature appear to be virtually independent

TABLE I

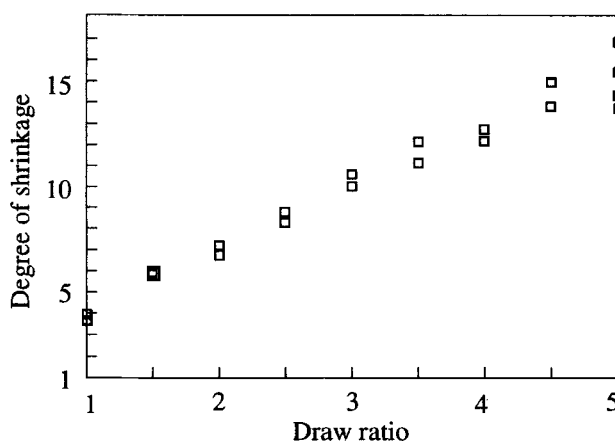| Draw ratio	χ_c (%)	T_m (°C)	$\langle P_2 \rangle$	$\langle P_4 \rangle$
1	69.1	235.7	0.981	0.937
1.5	70.8	236.9		
2	71.7	237.3 (239.5)	0.985	0.950
2.5	70.3	237.3		
3	73.3	236.5	0.986	0.954
3.5	74.5	235.9 (238.5)		
4	69.0	236.4 (238.7)	0.988	0.960
4.5	72.1	235.7 (240.7)		
5	74.1	239.1 (241.3)	0.991	0.970

FIGURE 2   Degree of shrinkage (the length before shrinking divided by the length after shrinking at 250°C) as a function of the draw ratio.

of the draw ratio. The average values obtained are $72\pm2\%$ for the crystallinity and $237\pm1\,°C$ $(240\pm1\,°C)$ for the peak melting temperature, the value indicated between brackets being the average peak value of a second melting peak which was obtained in some cases.

Also shown in Table I are the values of the second- and fourth-rank order parameters as obtained from WAXS. The crystalline order is practically maximum already at a draw ratio of 1 and increases only slightly further with draw ratio.

Figure 3 shows the birefringence as a function of the draw ratio. The indicated error is the error in the average of four measurements. The birefringence was calculated using the diameter as determined from the *dtex*. A slight but significant increase in the birefringence can be observed with increasing draw ratio. Particularly noteworthy is the fact that the birefringence is already relatively high at a draw ratio of 1 (passed through the oven). This is partly attributable to the effects of prestretching (the birefringence of the unstretched fiber is $(26.4\pm0.6)\times10^{-3}$), but also to the fact that the heat treatment under tension (a draw ratio of 1) causes the degree of orientational order to increase. The WAXS diffractograms show substantial differences between the fiber before and after this heat treatment. The crystalline orientational order parameter, f_c, is almost maximum already at a draw ratio of 1. Since the crystallinity does not change very much with draw ratio, it must be concluded that the
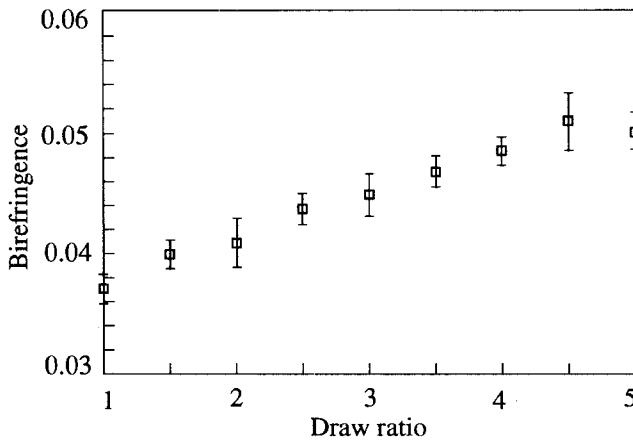
FIGURE 3   Birefringence as a function of the draw ratio.

increase in birefringence is virtually solely the result of an increase in the amorphous order parameter, f_a; see Equation (2). If we use the published value of $n_c^0 = 51.8 \times 10^{-3}$ for the intrinsic birefringence of the crystalline phase[11] and substitute 0.72 for χ_c in Equation (2), we arrive at an amorphous order parameter, f_a, of close to 0 for a draw ratio of 1. This is indeed what one would expect, because the increase in the degree of crystalline order and crystallinity that occurs in the heat treatment under tension will be accompanied by orientational relaxation in the amorphous phase.

Calculations

With the aid of Equation (2) it is possible to determine the amorphous order parameter for different draw ratios if the intrinsic birefringence values Δn_c^0 and Δn_a^0 are known. Values have indeed been reported in the literature:[11] 51.8×10^{-3} for Δn_c and 43.8×10^{-3} for Δn_a^0. For $\chi_c = 0.72$ and $f_c = f_a = 1$ these values suggest that the birefringence, Δn, never exceeds 49.6×10^{-3}, whereas values of 51×10^{-3} are already obtained at (non-ultimate) draw ratios (Figure 3). Furthermore, the fully drawn yarn was found to have a birefringence of $(56.9 \pm 1.6) \times 10^{-3}$, which is among the highest values ever reported. This means that at least one of these intrinsic values is not correct. In the present report we will assume that the value of the crystalline intrinsic birefringence is possibly correct and that the amorphous phase value is not. Indeed, as explained in Reference 11, the value for the crystalline intrinsic birefringence was obtained experimentally and was also calculated from reported bond polarizabilities. However, the experimentally determined amorphous intrinsic birefringence depended on the values obtained for the amorphous order parameter using an indirect method such as fluorescence depolarization, which means that this value may be suspect.

If the increase in the degree of amorphous order is the main cause of the increase in birefringence, then there must also be a connection between the increase in birefringence and the increase in strength and modulus.

Figure 4 shows the relation between the modulus and the birefringence. We observe a linear relationship between $1/E$ and Δn, as already predicted in Equation (5). A least squares adjustment yields $a = 0.157 \pm 0.002$ and $b = 2.61 \pm 0.16$.
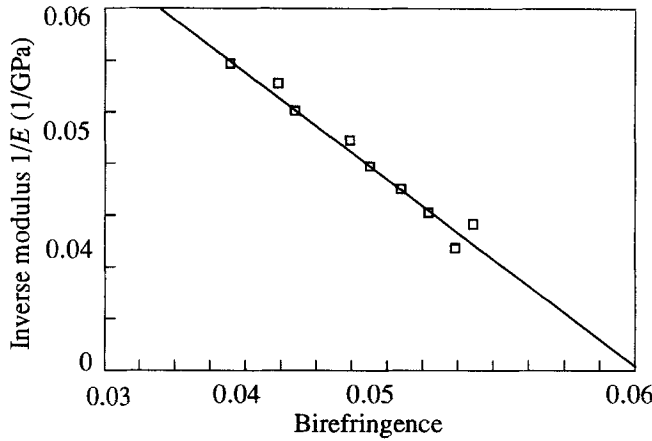
FIGURE 4   Relation between modulus and birefringence. The straight line expresses the linear relationship between $1/E$ and Δn.

Two simple extrapolations can now be derived. If we assume that the system is homogeneous (consisting of one phase) then the modulus for the isotropic material ($\Delta n = 0$) is 6.4 GPa. In addition, a maximum birefringence value can be obtained for $1/E \to 0$: $\Delta n_{max} = 60.2 \times 10^{-3}$. Although a maximum birefringence value of 63×10^{-3} was reported in the literature,[12] a much lower maximum value is usually used for orientation measurements.[13,14] The value of 51.8×10^{-3} already mentioned above for the intrinsic birefringence of the crystals need not conflict with the higher value found for the measured birefringence: the intrinsic birefringence of the amorphous phase may be much higher than that of the crystalline phase, as indeed turns out to be the case with polyethylene and polypropylene.[15,16]

On the basis of a crystalline-amorphous two-phase model in series it is possible to correlate measurements of the modulus and the birefringence according to Equation (6). By substituting[17] an average value of $f_c = \langle P_2 \rangle = 0.986$, $\langle P_4 \rangle = 0.954$, $\Delta n_c^0 = 51.8 \times 10^{-3}$, $\chi_c = 0.72$, and $S_{11} = 0.0687$ GPa^{-1}, $S_{13} = -0.003$ GPa^{-1}, $S_{33} = 0.0035$ GPa^{-1}, and $S_{44} = 0.0928$ GPa^{-1}, the following can be determined from the slope and intercept of the linear fit:

$$n_a^0 = 0.079 \pm 0.009$$
$$E_{iso} = 4.8 \pm 0.5 \text{ GPa}.$$

From Equation (3) and the value measured for the modulus it follows that the value of E_a at a draw ratio of 1 is 5.5 GPa, close to the value of the isotropic state, which confirms the aforementioned statement that the amorphous phase is not very ordered at a draw ratio of 1 ($E_a \approx E_{iso}$). Since the mechanical testing was performed straight after the hot drawing of the fibers, all values of the amorphous moduli refer to the dry state. Absorption of water will lower these values.

A second estimate of δn_a^0 can be made by assuming that the value found for the maximum birefringence (through extrapolation to $1/E \to 0$ in Figure 4) is found for $f_a = 1$ at a crystallinity of 72%. In that case $\Delta n_a = 82 \times 10^{-3}$ is obtained with the aid of Equation (2), i.e. practically the same value as that obtained from the calculation above.
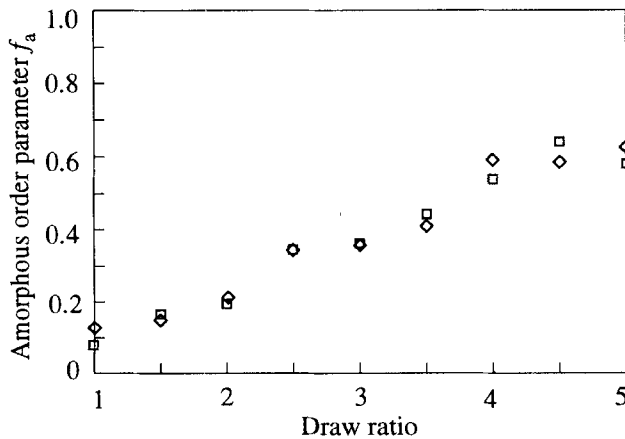
FIGURE 5   Order parameter f_a of the amorphous phase as a function of the draw ratio. $\square$, determined from Equations (3) and (4); $\lozenge$, determined from Equation (2).

Values of between 3.8 and 6.1 GPa have been reported in the literature for the amorphous modulus of isotropic PVAL.[18] These are based on a series model and known crystallinity and crystalline modulus values.

From the measured modulus values, the amorphous modulus, E_a follows as a function of the draw ratio using Equation (3). E_a increases from 5.5 GPa for a draw ratio of 1 to 12.9 GPa for a draw ratio of 5.

Amorphous order

If we assume that the value of 79×10^{-3} found for Δn_a^0 is correct, then it is possible to determine the amorphous order parameter, f_a, as a function of the draw ratio with the aid of Equation (2), using the individual values for χ_c and f_c. It is also possible to calculate f_a using Equations (3) and (4) and the value of $E_{iso} = 4.8$ GPa. Both results are shown in Figure 5. Errors in these results are estimated to be around 0.06. It should be born in mind, however, that the intrinsic amorphous birefringence may not always be constant and can be dependent on the amorphous order parameter itself.[16] For the present investigation we will not explore this phenomenon any further and will simply assume Δn_a^0 to be constant.

If we take a look at the order parameters of the crystalline and the amorphous fraction, we see that a strange deformation mechanism occurs in the drawing of these PVAL fibers. The crystallinity and crystalline orientation do not change (or change only very little), whereas the amorphous phase shows a marked increase in orientational order. The average chain orientation does not follow the usual pseudo-affine deformation model,[10] as can be seen in Figure 6, where the birefringence is plotted against the draw ratio as obtained from shrinkage experiments. It should be noted that the results were not obtained during a deformation experiment, but after separate drawing steps, in each of which the fibers were cooled to room temperature under tension. This means that the observed deformation pattern also represents the thermal history of the fibers, including partial melting during the hot drawing and crystallization under tension.
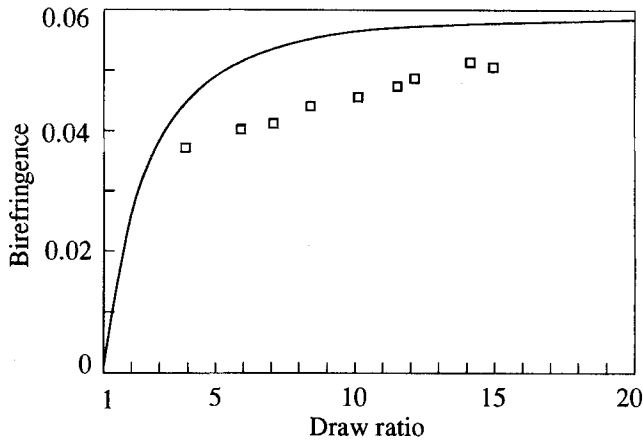
FIGURE 6   Birefringence as a function of draw ratio as obtained from shrinkage experiments. The drawn curve represents the birefringence that follows from the pseudo-affine deformation model with a maximal value of $\Delta n = 0.060$.
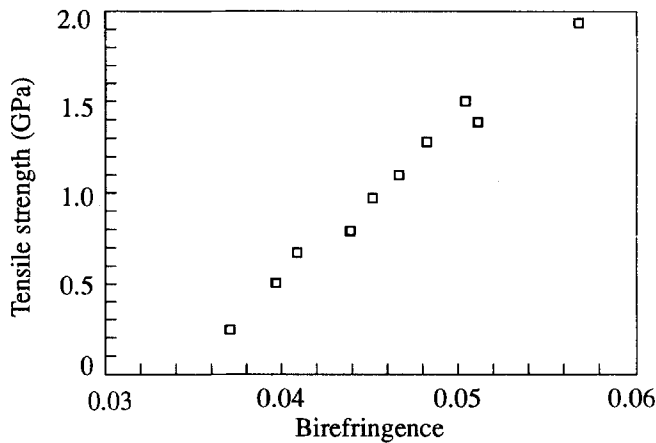
FIGURE 7   Relation between tensile strength and birefringence.

Tensile strength

Figure 7 shows the tensile strength as a function of the birefringence. We observe a linear relationship between the two parameters. Surprisingly, we found a similar linear relationship when we replotted the tensile strength and birefringence data of Kunugi *et al.*[5] and Tanaka *et al.*:[19] after we had reduced their values for the tensile strength by 15% (which is approximately the difference in strength between a multifilament yarn and a monofilament), the various data followed more or less the same linear curve. Figure 7 also contains the birefringence and tensile strength values of the one fully drawn yarn, which lie on the same line.

Figure 8 shows the tensile strength as a function of the amorphous order parameter f_a. The direct correlation is clear. A simple linear extrapolation of these values leads to tensile strengths of $\sigma = 2.20 \pm 0.13$ GPa for $f_a = 1$ and $\sigma = 0.16 \pm 0.08$ GPa for $f_a = 0$.
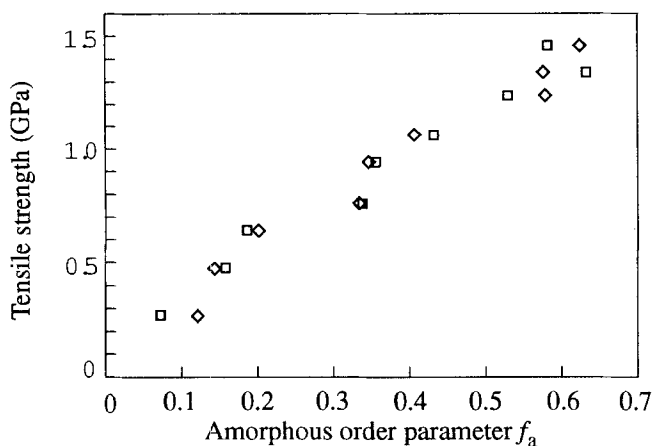
FIGURE 8   Relation between tensile strength and the amorphous order parameter f_a. □, determined from Equations (3) and (4); ◊, determined from Equation (2).

Now that we have seen that the increase in tensile strength correlates well with an increase in the degree of amorphous order, the next question is whether there is a causal connection between the two. In theory, an isolated chain will break when it is stretched too far, irrespective of its original conformation. Orientation alone lowers the elongation at break, but does not influence the tensile strength. In a real material, rupture is thought to occur at positions were the local stress exceeds the strength at break of a polymer chain, which means that a homogeneous stress distribution favors high tensile strengths.[20,21] It is interesting to note that the amorphous draw ratio at the time of break (calculated from the amorphous order parameter using the pseudo-affine deformation model and the draw ratio related to the elongation at break) is higher at higher draw ratios. One could now argue that an increase in the stress applied to the (amorphous) material causes a decrease in the width of the stress distribution. Such homogenization as a result of stretching could be thought of as a process in which chain or microfibril slippage occurs, which leads to a reduction of the most stressed chains after cooling.

Two-phase model

One of the concluding remarks should be that in the case of PVAL fibers the assumption of a two-phase crystalline-amorphous series model has proven to be very useful. This is probably because the draw ratios of PVAL fibers are relatively low compared with those of gel-spun polyethylene fibers. In the latter case substantial amounts of crystalline tie molecules crossing the amorphous phase is thought to result in superior properties.[22] It is realized that small amounts of tight chains crossing amorphous layers in PVAL fibers may influence the conclusions drawn above. These tie molecules may not be observed in a crystallinity or WAXS measurement, but may very well contribute to the mechanical properties. Following Penning et al.[22] and neglecting the contribution of the amorphous phase, the increase in modulus could also be explained by an increase in the fraction of taut tie molecules crossing the amorphous layers. Calculations show that in such a case up to 5% of the amorphous phase has to consist of such tight chains. Such an increase, however, was not observed in the crystallinity measurements and could furthermore not

account for the increase in birefringence that was found. A combination of both effects would lead to lower isotropic amorphous modulus values, but to even higher intrinsic amorphous birefringence values.

CONCLUSION

Both the tensile strength and modulus of gel-spun PVAL fibers correlate with the amorphous orientational order parameter f_a.

The birefringence of the fibers is the total of a crystalline and an amorphous component with intrinsic birefringence values of 52×10^{-3} and 79×10^{-3}, respectively.

The modulus of the dry isotropic amorphous phase of PVAL is 4.8 GPa.

The mechanical properties and birefringence of PVAL fibers can be well explained on the basis of a two phase crystalline-amorphous series model.

Acknowledgments

References

1. I. Sakurada, *Polyvinyl Alcohol Fibers*, (Marcel Dekker, New York, 1985).
2. P. Smith, P. J. Lemstra, B. Kalb, and A. J. Pennings, *Polym. Bull.*, **1**, 733 (1979).
3. P. D. Garrett and D. T. Grubb, *J. Mater. Res.*, **1**, 861 (1986).
4. K. Yamaura, T. Tanigami, N. Hayashi, K.-I. Kosuda, S. Okuda, Y. Takemura, M. Itoh, and S. Matsuzawa, *J. Appl. Polym. Sci.*, **40**, 905 (1990).
5. T. Kunugi, T. Kawasumi, and T. Ito, *J. Appl. Polym. Sci.*, **40**, 2101 (1990).
6. R. Schellekens and C. Bastiaansen, *J. Appl. Polym. Sci.*, **43**, 2311 (1991).
7. P. H. Hermans, *Contribution to the Physics of Cellulose Fibres*, (Elsevier, Amsterdam, 1946).
8. I. M. Ward, *Developments in Oriented Polymers-I*, Ed. I. M. Ward, (Appl. Sci. Publishers, London, 1982), p. 153.
9. L. C. E. Struik, *Internal Stresses, Dimensional Instabilities and Molecular Orientations in Plastics*, (Wiley, Chichester, 1990).
10. I. M. Ward, *Proc. Phys. Soc.*, **80**, 1176 (1962).
11. S. Hibi, M. Maeda, M. Takeuchi, S. Nomura, Y. Shibata, and H. Kawai, *Sen-i Gakkaishi*, **27**, 41 (1970).
12. A. D. Gabaraeva, M. F. Milagin, and N. I. Shishkin, *Mekh. Polim.*, **3**, 726 (1967).
13. S. Nomura and H. Kawai, *J. Polym. Sci.: Part A-2*, **4**, 797 (1966).
14. M. Shibayama, H. Kurokawa, S. Nomura, S. Roy, R.S. Stein, and W. Wu, *Macromolecules*, **23**, 1438 (1990).
15. M. Pietralla, H.-P. Grossman, and J. K. Krüger, *J. Polym. Sci., Polym. Phys. Ed.*, **20**, 1193 (1982).
16. A. R. Wedgewood and J. C. Seferis, *Polym. Eng. Sci.*, **24**, 328 (1984).
17. K. Tashiro, M. Kobayashi, and H. Tadokoro, *Macromolecules*, **11**, 914 (1978).
18. K. E. Perepelkin, *Angew. Makromol. Chem.*, **22**, 181 (1972).
19. H. Tanaka, M. Suzuki, and F. Ueda, *EP*, 0 146 084 (1988).
20. L. I. Slutsker, *J. Polym. Sci., Polym. Phys. Ed.*, **22**, 805 (1984).
21. A. Peterlin, *Monogr. Textb. Mater. Sci.*, **8**, 491 (1976).
22. J. P. Penning, H. van der Werff, M. Roukema, and A. J. Pennings, *Polym. Bull.*, **23**, 347 (1990).